significantly in going from the hydrogen-substituted complex to the methyl-substituted complex because of the hydrogen inductive through-bond electronic effect. Changes in the R1 and CE2 resonances should be more subtle as the substituent is changed from methyl to hydroxyethyl to benzyl since steric interactions are expected play a more prominent role.

These trends are well evidenced by the stick diagram of the methylene carbon peaks shown in Figure 8. The three methylene carbons about N2 exhibit approximately the same chemical shifts for all four complexes. The R1 and CE1 carbons are shifted dramatically downfield in going from the *N*-hydrogen to the *N*-methyl complex. These two peaks gradually shift slightly upfield as the N-substituent size is increased.

The trends observed here are completely analogous to those observed for the other series of N-substituted ed3a complexes of cobalt(III) with nitro, aqua, and cyano groups in the sixth coordinating position, as may be observed in Table VI.

Registry No. ed3a, 688-57-3; med3a, 40423-02-7; bed3a, 65311-06-0; Na[Co(med3a)NCS], 104393-76-2; Na[Co(hed3a)NCS], 104485-18-9; Na[Co(bed3a)NCS], 104393-77-3; [Co(ed3a)NCS]$^-$, 104393-78-4; [Co(ed3a)CN]$^-$, 104393-79-5; [Co(med3a)CN]$^-$, 104393-80-8; [Co(ed3a)NO_2]$^-$, 28459-67-8; [Co(med3a)NO_2]$^-$, 33972-16-6; [Co(hed3a)NO_2]$^-$, 33972-17-7; [Co(bed3a)NO_2]$^-$, 72513-55-4; [Co(ed3a)H_2O], 26599-29-1; [Co(med3a)H_2O], 33972-19-9; [Co(hed3a)H_2O], 33972-21-3; [Co(bed3a)H_2O], 72513-56-5; ethylenediamine-*N*,*N*'-diacetic acid, 5657-17-0; sodium chloroacetate, 3926-62-3; *N*-methylethylenediamine, 109-81-9; *N*-benzylethylenediamine, 4152-09-4.

Contribution from the Institut für Anorganische Chemie, TH Aachen, D-5100 Aachen, FRG, Institut für Anorganische Chemie, TU Clausthal, D-3392 Clausthal-Zellerfeld, FRG, and Anorganische Chemie, Fachbereich 9, BUGH, D-5600 Wuppertal 1, FRG

Organometallic S,S Ligands with π-Donor Properties. Structure and Magnetism of $[\{(C_5H_5)Ni[P(S)(OCH_3)_2]_2\}_2Ni]$, a Complex with Tetrahedral NiS_4 Coordination

Wolfgang Kläui,*[1a] Karin Schmidt,[1a] Anja Bockmann,[1a] David J. Brauer,*[1b] Jochen Wilke,[1b] Heiko Lueken,*[1a] and Ulrich Elsenhans[1c]

Received March 20, 1986

The sodium salts of the organometallic anions $L^- = [(C_5H_5)Ni\{P(S)R_2\}_2]^-$, R = OCH_3, CH_3, react as S,S-chelate ligands with transition-metal ions M_{aq}^{2+} = Mn^{2+}, Fe^{2+}, Co^{2+}, Ni^{2+}, Zn^{2+}, Cd^{2+}, Hg^{2+} to give tetrahedral ML_2 complexes. Reactions of L^- with $[PdCl_2(C_6H_5CN)_2]$, CH_3HgCl, and $Bi(NO_3)_3 \cdot 5H_2O$ yield planar PdL_2, CH_3HgL, and $[BiL_2]NO_3$, respectively. No ML_3 complexes could be synthesized. Crystals of $[\{(C_5H_5)Ni[P(S)(OCH_3)_2]_2\}_2Ni]$ belong to the monoclinic space group $C2/c$ with a = 19.108 (2) Å, b = 8.8044 (8) Å, c = 18.663 (1) Å, β = 102.683 (6)°, and Z = 4. Refinement converged with a conventional R value of 0.031 for 3878 reflections with $F \geq 4\sigma(F)$. The trinuclear structure possesses two terminal $(C_5H_5)Ni$ fragments. Each of these enters two Ni–P bonds averaging 2.1363 (4) Å. The central Ni atom, which is located on a crystallographic twofold axis, bonds to a distorted tetrahedral array of four S atoms. The two crystallographically independent Ni–S distances are significantly different, and the S–Ni–S bond angles vary from 97.74 (2) to 138.25 (3)°. The magnetism μ_{eff} of FeL_2 (4.7 μ_B (μ_B = Bohr magneton)), CoL_2 (4.3 μ_B), and NiL_2 (2.9 μ_B), R = OCH_3, has been determined in methylene chloride solution. The temperature-dependent magnetic moment of NiL_2, R = OCH_3, in the solid state (μ_{eff}(3.8 K) ≈ 1.9 μ_B, μ_{eff}(298 K) ≈ 3.3 μ_B) can roughly be interpreted in terms of a tetrahedral NiS_4 model. It is postulated that the ligands L^- are good π-donors and that it is this property which favors the tetrahedral over planar NiS_4 coordination.

Introduction

Ligands with sulfur donor atoms are unique in the sense that they cannot be assigned a characteristic position in the spectrochemical series I < Cl < O < N < C.[2] Jørgensen has shown that the ligand field strength of sulfur donors covers a remarkable range beginning at that of chloride, traversing that of oxygen ligands and ending at that of alkylamines.[3] In terms of ligand field theory this means that the relative σ-donor and π-acceptor vs. π-donor properties are particularly variable. As a consequence of this the coordination chemistry of sulfur ligands is remarkably many-sided.[4] We have recently described the synthesis of a new type of S,S-chelate ligand **3a,b**.[5,6] The zinc complexes **2a,b** were prepared via eq 1 and 2, and the sodium salts **3a,b** of these organometallic S,S-chelate ligands were obtained from **2a,b** via eq 3.

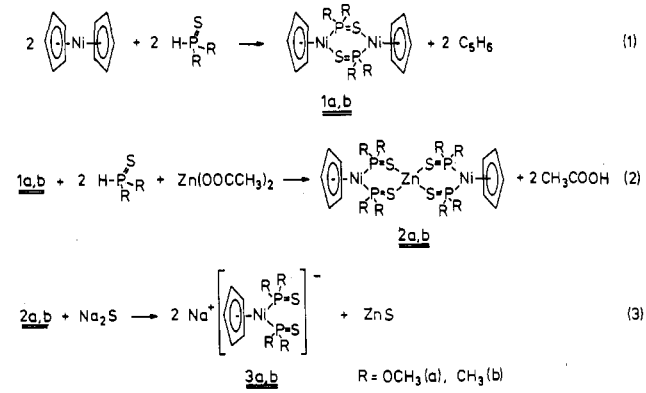

Now we have studied the coordination chemistry of these novel ligands in order to characterize their steric and electronic properties. We expected that the coordination chemistry of the S,S-chelates **3** would resemble that of dithioacetylacetonate (SacSac) since the O,O-chelate ligands $[(C_5H_5)Ni\{P(O)R_2\}_2]^-$, which are homologous to **3**, have been reported to possess a coordination chemistry which is similar to that of acetylacetonate.[7] The preparation and properties of metal complexes of the S,S-chelates **3**, which are reported below, demonstrate that their electronic properties differ drastically from those of SacSac compounds.

(1) (a) TH Aachen. (b) BUGH Wuppertal. (c) TU Clausthal.
(2) Jørgensen, C. K. *Inorg. Chim. Acta Rev.* **1968**, *2*, 65.
(3) Jørgensen, C. K. *J. Inorg. Nucl. Chem.* **1962**, *24*, 1571.
(4) Raper, E. S. *Coord. Chem. Rev.* **1985**, *61*, 115 and the reviews cited as ref 1–23 therein.
(5) Kläui, W.; Eberspach, W.; Schwarz, R. *J. Organomet. Chem.* **1983**, *252*, 347.
(6) Kläui, W.; Schmidt, K.; Bockmann, A.; Hofmann, P.; Schmidt, H. R.; Stauffert, P. *J. Organomet. Chem.* **1985**, *286*, 407.
(7) Werner, H.; Ngo-Khac, T.; Friebel, C.; Köhler, P.; Reinen, D. *Z. Naturforsch., B: Anorg. Chem., Org. Chem.* **1981**, *36B*, 322.

0020-1669/86/1325-4125$01.50/0

Table I. Crystal Data and Data Collection Parameters

formula	$C_{18}H_{34}Ni_3O_8P_4S_4$
M_r	806.75
space group	$C2/c$
a, Å	19.108 (2)
b, Å	8.8044 (8)
c, Å	18.663 (1)
β, deg	102.683 (6)
Z	4
d(calcd), g cm^{-3}	1.75
cryst dimens, mm	0.27 × 0.35 × 0.88
radiation (λ, Å)	Mo Kα (0.71073, Zr filtered)
temp, °C	23(1)
no. of reflcns	
collcd	4851
unique	4450
used in refinement with $F \geq 4\sigma(F)$	3878
rel transmission factors	0.574–0.428
μ(Mo Kα), cm^{-1}	23.4
$R = \sum\Delta/\sum\|F_o\|$	0.031
$R_w = [\sum w\Delta^2/\sum w\|F_o\|^2]^{1/2}$	0.050

Experimental Section

Dimethylphosphine sulfide,[8] diphenylphosphine sulfide,[9] *O,O'*-dimethyl thiophosphite,[10] $[\{(C_5H_5)NiP(S)R_2\}_2]$ (R = OCH_3, CH_3; **1a,b**),[5] and the sodium salts of the S,S-chelate ligands $[(C_5H_5)Ni\{P(S)R_2\}_2]^-$ (**3a**, R = OCH_3;[5] **3b**, R = CH_3[6]) were prepared according to the published procedures. All manipulations were carried out under dry nitrogen in Schlenk glassware.

The elemental analyses were obtained from Analytical Laboratories, D-5250 Engelskirchen, FRG. All new compounds gave satisfactory elemental analyses. ^1H and ^{31}P NMR spectra were recorded on Bruker WP-80-FT and WH-270-FT spectrometers. The magnetic susceptibilities of samples in solution were determined by the Evans method.[11] Variable-temperature (3.8–300 K) magnetic susceptibility measurements on powdered samples (weighed portions of 9–10 mg) were carried out by using a Faraday balance with $HgCo(SCN)_4$ as standard.[12] Susceptibilities were corrected for the diamagnetism of the molecular system (χ_{dia} = −45 × 10^{-11} m^3 mol^{-1}, SI units), determined by susceptibility measurements of the potassium salt of the ligand **3a**, $K[(C_5H_5)Ni\{P(S)(OCH_3)_2\}_2]$.

X-ray Diffraction. The crystal data and data collection parameters are given in Table I. X-ray powder diffraction data were obtained with a Guinier-Simon camera using Cu $K\alpha_1$ radiation. The crystal used in the X-ray structure determination of $[\{(C_5H_5)Ni[P(S)(OCH_3)_2]\}_2Ni]$ (**4a**) was mounted in a thin-walled glass capillary under argon. The symmetry and systematic absences revealed by Weissenberg photographs were indicative of the space groups *Cc* and *C2/c*. Further measurements were made with a Siemens AED-1 diffractometer employing Mo Kα radiation. The lattice constants were derived from the Bragg angles of 59 centered reflections. Intensity data (hkl, $\bar{h}kl$, $4 < 2\theta < 60°$) were collected by the ω–2θ step scan technique. Between 54 and 64 steps ($\Delta\omega$ = 0.02°, $\Delta 2\theta$ = 0.04°) of 0.61 s duration were used, depending on the Bragg angle—the peaks falling in the middle two-thirds of the scan range. If the initial pass yielded an $I/\sigma(I)$ ratio between 2 and 25, then the reflection was remeasured and the two results were summed. Remeasurement was made with an attenuated primary beam if the maximum intensity exceeded 6000 counts/s. System stability was checked by hourly monitoring of three standard reflections. The data were corrected for the slight drift of the standards (<2.4%).

The coordinates of the Ni, P, and S atoms were obtained by multisolution direct methods, and the remaining non-hydrogen atoms were located with a Fourier synthesis. After these atoms were refined anisotropically, the H atoms were taken from a difference Fourier map and their coordinates were idealized (C–H 0.95 Å, cyclopentadienyl H's riding on the external bisectors of the C–C–C angles, methyls refining as rigid groups with 109.5° H–C–H angles). The H atoms of the same organic group were assigned common isotropic thermal parameters. Least-squares refinement of the structure minimized the function $\sum w\Delta^2$, where $w^{-1} = (\sigma^2(|F_o|) + 0.0004|F_o|^2)$ and $\Delta = ||F_o| - |F_c||$. Convergence, $|\xi/\sigma|_{max}$ = 0.09, was reached with $R = \sum\Delta/\sum|F_o|$ = 0.031 and R_w = $[\sum w\Delta^2/\sum w|F_o|^2]^{1/2}$ = 0.050 for the observed reflections. These residuals are 0.037 and 0.051, respectively, for all reflections. The final difference Fourier synthesis, 0.90 to −0.45 e/Å^3, contained no chemically significant

Table II. Positional Parameters of the Non-Hydrogen Atoms in $[\{(C_5H_5)Ni[P(S)(OCH_3)_2]\}_2Ni]$ (**4a**)

atom	x	y	z
Ni(1)	0.38466 (1)	0.29144 (3)	0.09778 (1)
Ni(2)	0.5000	0.10645 (4)	0.2500
S(1)	0.40309 (3)	0.19863 (7)	0.28850 (3)
S(2)	0.46130 (3)	−0.06593 (7)	0.15463 (3)
P(1)	0.35946 (3)	0.33147 (6)	0.20218 (3)
P(2)	0.37477 (3)	0.04983 (6)	0.09905 (3)
O(1)	0.27591 (9)	0.3210 (2)	0.2044 (1)
O(2)	0.3795 (1)	0.5062 (2)	0.2227 (1)
O(3)	0.30478 (9)	0.0056 (2)	0.1287 (1)
O(4)	0.3530 (1)	−0.0264 (3)	0.0191 (1)
C(1)	0.2260 (1)	0.4189 (4)	0.1585 (2)
C(2)	0.3728 (2)	0.5716 (4)	0.2908 (2)
C(3)	0.2853 (2)	−0.1487 (3)	0.1373 (2)
C(4)	0.3967 (2)	−0.1124 (4)	−0.0165 (2)
C(5)	0.4181 (2)	0.3109 (3)	−0.0004 (1)
C(6)	0.4675 (2)	0.3890 (3)	0.0531 (2)
C(7)	0.4287 (2)	0.5000 (3)	0.0803 (2)
C(8)	0.3563 (2)	0.4970 (4)	0.0400 (2)
C(9)	0.3504 (2)	0.3811 (4)	−0.0110 (1)

Table III. Selected Bond Distances (Å) in $[\{(C_5H_5)Ni[P(S)(OCH_3)_2]\}_2Ni]$ (**4a**)

Ni(2)–S(1)	2.2778 (6)	C(8)–C(9)	1.383 (5)
Ni(2)–S(2)	2.3324 (6)	C(9)–C(5)	1.408 (4)
Ni(1)–P(1)	2.1364 (6)	P(1)–S(1)	2.0170 (8)
Ni(1)–P(2)	2.1362 (6)	P(2)–S(2)	2.0237 (8)
Ni(1)–C(5)	2.075 (3)	P(1)–O(1)	1.609 (2)
Ni(1)–C(6)	2.125 (3)	P(1)–O(2)	1.611 (2)
Ni(1)–C(7)	2.075 (3)	P(2)–O(3)	1.603 (2)
Ni(1)–C(8)	2.115 (3)	P(2)–O(4)	1.606 (2)
Ni(1)–C(9)	2.143 (3)	O(1)–C(1)	1.424 (3)
C(5)–C(6)	1.395 (4)	O(2)–C(2)	1.426 (4)
C(6)–C(7)	1.388 (5)	O(3)–C(3)	1.427 (3)
C(7)–C(8)	1.422 (5)	O(4)–C(4)	1.397 (3)

Table IV. Selected Bond Angles (deg) in $[\{(C_5H_5)Ni[P(S)(OCH_3)_2]\}_2Ni]$ (**4a**)

S(1)–Ni(2)–S(2)	109.21 (2)	P(1)–Ni(1)–P(2)	96.66 (2)
S(1)–Ni(2)–S(1)'[a]	138.25 (3)	O(1)–P(1)–O(2)	103.5 (1)
S(1)–Ni(2)–S(2)'	97.74 (2)	O(3)–P(2)–O(4)	98.8 (1)
S(2)–Ni(2)–S(2)'	98.81 (2)	C(6)–C(5)–C(9)	109.9 (3)
S(1)–P(1)–Ni(1)	119.76 (3)	C(5)–C(6)–C(7)	106.1 (3)
S(2)–P(2)–Ni(1)	116.29 (3)	C(6)–C(7)–C(8)	109.2 (3)
P(1)–S(1)–Ni(2)	100.18 (3)	C(7)–C(8)–C(9)	107.5 (3)
P(2)–S(2)–Ni(2)	98.62 (3)	C(5)–C(9)–C(8)	107.0 (3)

[a] Coordinates of primed atoms are related to those in Table I by x', y', $z' = 1 - x, y, 0.5 - z$.

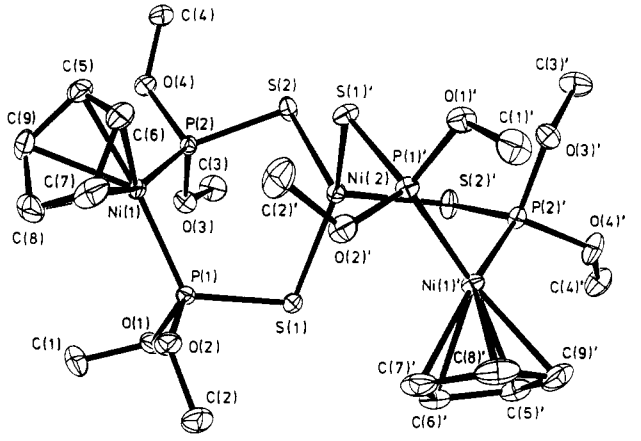

Figure 1. Perspective drawing of $[\{(C_5H_5)Ni[P(S)(OCH_3)_2]\}_2Ni]$ (**4a**) with 20 % probability thermal ellipsoids.

(8) Sasse, K. In *Houben-Weyl Methoden der organischen Chemie*; Georg Thieme: Stuttgart, 1964; Vol. XII/1, p 212.
(9) Peters, G. *J. Am. Chem. Soc.* **1960**, *82*, 4751.
(10) Schliebs, R. Ger. Offen. 1768503.
(11) Evans, D. F. *J. Chem. Soc.* **1959**, 2003.
(12) Lueken, H.; Rohne, W. *Z. Anorg. Allg. Chem.* **1975**, *418*, 103.

features. An extinction correction of the form $F_c = F_c'(1-\chi F_c'^2/(\sin\theta))$, $\chi = 4.1\ (4) \times 10^{-8}$, was applied. Dispersion corrected, relativistic Hartree–Fock scattering factors were used for all atoms except H (SDS).[13] Coordinates of the non-hydrogen atoms are given in Table II, and the numbering scheme is defined in Figure 1. All calculations were made assuming space group C2/c, the choice being confirmed by the refinement. SHELX-76,[14] ORTEP,[15] PARST,[16] and several local programs were used. Bond distances and angles are given in Tables III and IV, respectively.

Preparations. Bis[(cyclopentadienyl)bis(*O*,*O*'-dimethyl thiophosphito-*P*)nickelato-*S*,*S*']nickel(II) (4a). The addition of 155 mg (0.39 mmol) of NaL (**3a**) in 5 mL of methanol to a solution of 46 mg (0.19 mmol) of $NiCl_2 \cdot 6H_2O$ in 5 mL of methanol caused the immediate formation of a dark green precipitate. The product was filtered off, washed with methanol (two 10-mL portions), and dried. Recrystallization from methylene chloride/diethylether gave dark green crystals; yield 135 mg (87%). Dec pt: 112–117 °C. ^{1}H NMR (CD_2Cl_2): δ 4.7 (s, br, OCH_3), 2.6 (s, br, C_5H_5). The magnetic moments are 3.26 (solid, 23 °C) and 2.9 μ_B (CH_2Cl_2 solution, 25 °C). The solid is air stable, but in solution the complex rapidly decomposes.

Bis[(cyclopentadienyl)bis(dimethylthiophosphinito-*P*)nickelato-*S*,*S*']nickel(II) (4b) was prepared in the same manner as **4a** from 160 mg (0.48 mmol) of NaL (**3b**) and 70 mg (0.29 mmol) of $NiCl_2 \cdot 6H_2O$; yield 76 mg, (45%). ^{1}H NMR (CD_2Cl_2): 4.7 (s, br, C_5H_5), 4.6 (s, br, CH_3).

Bis[(cyclopentadienyl)bis(*O*,*O*'-dimethyl thiophosphito-*P*)nickelato-*S*,*S*']palladium(II) (5a) was prepared in the same manner as **4a** from 223 mg (0.56 mmol) of NaL (**3a**) and 107 mg (0.28 mmol) of *trans*-$[PdCl_2(C_6H_5CN)_2]$; yield 120 mg (50%). The air-stable dark green crystals decompose at 119–120 °C. The compound is insoluble in methanol and ether and soluble in acetone and toluene; it decomposes slowly in chloroform. ^{1}H NMR ($CDCl_3$): δ 5.3 (t, ^3J(PNiCH) = 0.8 Hz, C_5H_5), 3.6 (virt t, ^3J(POCH) $\approx$ 13 Hz, OCH_3).

Bis[(cyclopentadienyl)bis(dimethylthiophosphinito-*P*)nickelato-*S*,*S*']palladium(II) (5b) was prepared in the same manner as **4a** from 126 mg (0.38 mmol) of NaL (**3b**) and 73 mg (0.19 mmol) of *trans*-$[PdCl_2(C_6H_5CN)_2]$; yield 63 mg (45%) of air-stable dark green crystals. The compound decomposes slowly in solution. ^{1}H NMR ($CDCl_3$): δ 5.2 (s, C_5H_5), 1.8 (virt. t, ^2J(PCH) $\approx$ 9 Hz, CH_3).

Bis[(cyclopentadienyl)bis(*O*,*O*'-dimethyl thiophosphito-*P*)nickelato-*S*,*S*']cobalt(II) (6a) was prepared in the same manner as **4a** from 261 mg (0.66 mmol) of NaL (**3a**) and 78 mg (0.33 mmol) of $CoCl_2 \cdot 6H_2O$, yield 199 mg (75%), as dark green, air-stable crystals. The compound is insoluble in methanol and ether and soluble in acetone, toluene, and methylene chloride. Dec pt: 138–145 °C. The magnetic moment is 4.3 μ_B (CH_2Cl_2 solution, 25 °C).

Bis[(cyclopentadienyl)bis(*O*,*O*'-dimethyl thiophosphito-*P*)nickelato-*S*,*S*']iron(II) (7a). A 10-mL aliquot of water was added to 377 mg (0.95 mmol) of NaL (**3a**) and 168 mg (0.43 mmol) of $(NH_4)_2Fe(SO_4)_2 \cdot 6H_2O$, and the resulting suspension was stirred for 1 h. The oily product was washed twice with 10 mL methanol and dried. Recrystallization from methylene chloride/diethyl ether gave dark green air-stable crystals; yield 272 mg (79%). The solubility is like that of **6a**. Dec pt: 120–124 °C. The magnetic moment is 4.7 μ_B (CH_2Cl_2 solution, 25 °C). Mass spectrum (electron impact, 70 eV): *m/e* 802 (M^+).

Bis[(cyclopentadienyl)bis(*O*,*O*'-dimethyl thiophosphito-*P*)nickelato-*S*,*S*']manganese(II) (8a) was prepared in the same manner as **4a** from 157 mg (0.40 mmol) of NaL (**3a**) and 39 mg (0.20 mmol) of $MnCl_2 \cdot 4H_2O$; yield 145 mg (90%) of dark green, air-stable crystals. The solubility is like that of **6a**. Dec pt: 130–140 °C. Mass spectrum: *m/e* 801 (M^+).

Bis[(cyclopentadienyl)bis(*O*,*O*'-dimethyl thiophosphito-*P*)nickelato-*S*,*S*']cadmium(II) (9a). A mixture of 700 mg (1.41 mmol) of $[\{(C_5H_5)NiP(S)(OCH_3)_2\}_2]$ (**1a**), 562 mg (2.11 mmol) of $Cd(OOCCH_3)_2 \cdot 2H_2O$, and 443 mg (3.51 mmol) of *O*,*O*'-dimethyl thiophosphite, $HP(S)(OCH_3)_2$, was stirred in 15 mL of benzene for 5 h at 50–60 °C and then for 2 days at room temperature. The excess cadmium acetate was filtered off, the solution evaporated to dryness, and the crude product recrystallized from methylene chloride/diethyl ether; yield 850 mg (70%) of dark green, air-stable crystals. Dec pt: 150–155 °C. ^{1}H NMR ($CDCl_3$): δ 5.4 (t, ^3J(PNiCH) = 0.8 Hz, C_5H_5), 3.6 (virt t, ^3J(POCH) $\approx$ 13.5 Hz, OCH_3). ^{31}P{^{1}H} NMR (relative to H_3PO_4, $CDCl_3$): δ 181.2 (s). Mass spectrum: *m/e* 860 (M^+).

Bis[(cyclopentadienyl)bis(*O*,*O*'-dimethyl thiophosphito-*P*)nickelato-*S*,*S*']mercury(II) (10a) was prepared in the same manner as **4a** from 315 mg (0.79 mmol) of NaL (**3a**) and 128 mg (0.40 mmol) of $Hg(OOCCH_3)_2$; yield 205 mg (54%) of dark green, air-stable crystals. Dec pt: 140–142 °C. ^{1}H NMR ($CDCl_3$): δ 5.4 (t, ^3J(PNiCH) = 0.7 Hz, C_5H_5), 3.6 (virt t, ^3J(POCH) $\approx$ 13.4 Hz, OCH_3).

Bis[(cyclopentadienyl)bis(dimethylthiophosphinito-*P*)nickelato-*S*,*S*']mercury(II) (10b) was prepared in the same manner as **9a** from 400 mg (0.92 mmol) of $[\{(C_5H_5)NiP(S)(CH_3)_2\}_2]$ (**1b**), 217 mg (2.30 mmol) of dimethylphosphine sulfide, $HP(S)(CH_3)_2$, and 441 mg (1.38 mmol) of $Hg(OOCCH_3)_2$; yield 580 mg (77%) of dark green, air-stable crystals. Dec pt: 150–155 °C. ^{1}H NMR ($CDCl_3$): δ 5.2 (s, C_5H_5), 1.8 (virt t, ^2J(PCH) $\approx$ 9 Hz, CH_3).

Bis[(cyclopentadienyl)bis(*O*,*O*'-dimethyl thiophosphito-*P*)nickelato-*S*,*S*']bismuth(III) Nitrate (11a). A mixture of 300 mg (0.76 mmol) of NaL (**3a**) and 122 mg (0.25 mmol) of $Bi(NO_3)_3 \cdot 5H_2O$ in 5 mL of methanol was stirred for 2 h. The resulting red-brown suspension was cooled to −28 °C for 2 days and then filtered and the solid residue recrystallized from methanol; yield 127 mg (50%) of red-brown air-sensitive crystals. Dec pt: 84–92 °C. ^{1}H NMR ($CDCl_3$): δ 5.7 (s, C_5H_5), 3.7 (virt t, ^3J(POCH) $\approx$ 13.3 Hz, OCH_3).

Bis[(cyclopentadienyl)bis(*O*,*O*'-dimethyl thiophosphito-*P*)nickelato-*S*,*S*']bismuth(III) hexafluorophosphate (12a) was prepared in the same manner as **11a** from 623 mg (1.57 mmol) of NaL (**3a**), 430 mg (0.89 mmol) of $Bi(NO_3)_3 \cdot 5H_2O$ and a large excess of ammonium hexafluorophosphate; yield 560 mg (64%) of red-brown air-stable crystals. ^{1}H NMR (acetone-d_6): δ 5.9 (t, ^3J(PNiCH) = 1.2 Hz, C_5H_5), 3.8 (virt t, ^3J(POCH) $\approx$ 14.0 Hz, OCH_3). ^{31}P{^{1}H} NMR (relative to H_3PO_4, acetone-d_6): δ +169.5 (s, br), −141.6 (sept, ^1J(PF) = 292 Hz, PF_6). Molar conductivity Λ = 74 Ω^{-1} cm^2 mol^{-1} (0.8 × 10^{-3} *m* CH_3NO_2 solution).

[(Cyclopentadienyl)bis(*O*,*O*'-dimethyl thiophosphito-*P*)nickelato-*S*,*S*']methylmercury(II) (13a). A mixture of 192 mg (0.48 mmol) of NaL (**3a**) and 121 mg (0.48 mmol) of chloromethylmercury in 20 mL of ether was stirred for 12 h. The solution was filtered and the solvent evaporated until crystallization occurred. The solution was cooled to −20 °C, and the green crystals were filtered off, washed with pentane, and dried; yield 229 mg (81%) of air-stable crystals. Dec pt: 85–90 °C. ^{1}H NMR ($CDCl_3$): δ 5.2 (t, ^3J(PNiCH) = 0.8 Hz, C_5H_5), 3.5 (virt t, ^3J(POCH) $\approx$ 13 Hz, OCH_3), 1.0 (s, d, ^2J(HgCH) = 193.5 Hz, $HgCH_3$).

[(Cyclopentadienyl)bis(dimethylthiophosphinito-*P*)nickelato-*S*,*S*']methylmercury(II) (13b) was prepared in the same manner as **13a** from 231 mg (0.69 mmol) of NaL (**3b**) and 161 mg (0.64 mmol) of chloromethylmercury. The crude product was recrystallized twice from methylene chloride/ether; yield 188 mg (56%). ^{1}H NMR ($CDCl_3$): δ 5.2 (s, C_5H_5), 1.8 (virt t, ^2J(PCH) $\approx$ 9 Hz, PCH_3), 0.8 (s, d, ^2J(HgCH) = 165.6 Hz, $HgCH_3$).

Results and Discussion

Preparations. The sodium salts of the dark green sulfur ligands **3a,b** (hereafter abbreviated as L^-) react with ions M^{2+} = Mn^{2+}, Fe^{2+}, Co^{2+}, Ni^{2+}, Cu^{2+}, Zn^{2+}, Cd^{2+}, Hg^{2+} in water or aqueous methanol to give dark green or black precipitates. These products all have the composition ML_2 with the exception of M = Cu, where reduction to Cu^+ yields a mixture of products. The palladium complexes PdL_2 are best obtained from *trans*-$[PdCl_2(C_6H_5CN)_2]$ with **3a,b** in methanol. We have not been able to synthesize NiL_2 (**4a,b**) directly from **1a,b** and $Ni(OOCCH_3)_2$, analogous to the preparation of the zinc complexes **2** (eq 2), but the complexes CdL_2 (**9a**) and HgL_2 (**10a,b**) are accessible via this alternative route (see Experimental Section). All ML_2 compounds are soluble in methylene chloride and benzene. They decompose slowly in chloroform. Apart from complexes with divalent metal ions, which are discussed further below, we have also tried to synthesize derivatives of L^- with mono and trivalent ions. The synthesis of HL from NaL failed because of decomposition of the ligands in the presence of acids; however with the prototypical soft acid CH_3Hg^+, the very stable compounds $LHgCH_3$ (**13a,b**) are formed.

Attempts to synthesize compounds of the type ML_3 with M^{3+} = V^{3+}, Cr^{3+}, and Fe^{3+} were unsuccessful. Partial decomposition and concomitant formation of NiL_2 was observed. NaL (**3a**) reacts with bismuth nitrate in methanol to give $[BiL_2]^+$ salts (**11a**, **12a**). No BiL_3 could be prepared. This is surprising since the sterically even more demanding S,S-chelate ligand $[N\{P(S)Ph_2\}_2]^-$ is known to form the 3:1 complex with bismuth.[17] The molar

(13) *International Tables for X-ray Crystallography*; Kynoch: Birmingham, England, 1974; Vol. 4, Tables 2.2B and 2.3.1.
(14) Sheldrick, G. M. SHELX-76, Program for Crystal Structure Determination, Cambridge, 1976.
(15) Johnson, C. K. *ORTEP-II*, Report ORNL-5138; Oak Ridge National Laboratory: Oak Ridge, TN, 1976.
(16) Nardelli, M. *Comput. Chem.* **1983**, *7*, 95.
(17) Williams, D. J.; Quicksall, C. O.; Barkigia, K. M. *Inorg. Chem.* **1982**, *21*, 2097.

Table V. Comparison of Bond Angles (deg) in Paramagnetic NiS_4 Fragments

compound	symmetry-related pairs	angles bisected by C_2 axis	ref
$[\{(C_5H_5)Ni[P(S)(OCH_3)_2]\}_2Ni]$ (**4a**)	97.74 (2)	138.25 (3)	this work
	97.74 (2)	98.81 (2)	
	109.21 (2)		
	109.21 (2)		
$[\{N[P(CH_3)_2S]_2\}_2Ni]$ (**14**)	106.0 (1)	117.0 (1)	21
	106.8 (1)	111.5 (1)	
	107.3 (1)		
	108.4 (1)		
$[(C_6H_5)_4P]_2[(C_6H_5S)_4Ni]$ (**15**)	92.0 (2)	124.9 (2)	22
	92.7 (2)	117.9 (2)	
	116.3 (2)		
	115.4 (2)		

conductivity of **12a** in 10^{-3} *m* nitromethane solution, $\Lambda = 74\ \Omega^{-1}$ cm^2 mol^{-1}, is in accordance with the presence of monomeric $[BiL_2]^+$ cations in solution. The ^1H NMR spectra of **11a** and **12a** are, apart from a slight low-field shift of the signals, identical with the spectrum of ZnL_2 (**2a**),[5] indicating a regular tetrahedral coordination of bismuth on the NMR time scale.

Magnetism and Structure of ML_2 Compounds in Solution. We were surprised to note that not only the cobalt, iron, and manganese complexes (**6a**, **7a**, **8a**) but also the nickel compounds NiL_2 (**4a**,**b**) are paramagnetic as judged from their ^1H NMR spectra. The OCH_3 and C_5H_5 signals of NiL_2 (**4a**) do not show any marked deviation from Curie behavior in the temperature range +80 to −70 °C. A departure from Curie behavior would have been indicative of a planar–tetrahedral equilibrium.[18] The magnetic moments of NiL_2 (**4a**), CoL_2 (**6a**), and FeL_2 (**7a**) in solution determined by the Evans method at 25 °C are μ_{eff} = 2.9 (NiL_2), 4.3 (CoL_2), and 4.7 μ_B (FeL_2). The observed paramagnetism of NiL_2 in solution is in the range characteristic of "distorted-tetrahedral" Ni(II) complexes.[19] The paramagnetism of NiL_2 is observed in noncoordinating solvents like benzene or methylene chloride. This excludes the possibility that the paramagnetic species are five- or six-coordinate complexes formed from diamagnetic planar NiL_2 and donor solvent molecules. Since there is no concentration dependence of the magnetic moment of NiL_2, we can also exclude self-association with formation of five- and six-coordinate Ni(II) species in solution as a source of the observed paramagnetism. From this evidence we conclude that the NiL_2 complexes **4a**,**b**, and very probably CoL_2 (**6a**) and FeL_2 (**7a**), also exist as monomeric tetrahedral ML_2 complexes in solution. From X-ray powder photographs it is evident that the ML_2 complexes **2a**, **4a**, **6a**, **7a**, and **8a** have very similar solid-state structures, which differ from that of the palladium complex **5a**.

Crystal Structure of NiL_2 (4a). The coordination geometry of the central nickel atom of **4a** is the most pregnant structural feature (see Figure 1). This atom possesses crystallographic twofold symmetry and is coordinated *tetrahedrally* to four sulfur atoms. While the Ni(2)–S(1) bond is distinctly (0.0546 (8) Å) shorter than the Ni(2)–S(2) linkage, the mean Ni–S distance (2.31 (4) Å) may be compared to those of $[\{N[P(S)(CH_3)_2]_2\}_2Ni]$ (**14**, 2.28 (1) Å[21]) and $[P(C_6H_5)_4]_2[Ni(SC_6H_5)_4]$ (**15**, 2.29 (1) Å[22]). Compounds **14** and **15** appear to be the only other structurally characterized NiS_4 species that possess tetrahedrally coordinated nickel(II). As Churchill has noted, the Ni–S distances in these compounds are longer than in square-planar nickel(II) complexes.[21] Interestingly, shorter distances (2.19 (1) Å) were also found in $[\{(C_5H_5)_2Nb(SCH_3)_2\}_2Ni](BF_4)_2$, which supposedly contains nickel(0) bonded tetrahedrally to four sulfur atoms as well as to two niobium atoms.[23]

In **4a**, the geometry of the NiS_4 fragment is so distorted from tetrahedral symmetry that only one of the symmetry elements of the tetrahedral point group, the C_2 axis, has been preserved. Thus the descent in symmetry is much greater than the prediction from the Jahn–Teller theory ($T_d \rightarrow D_{2d}$) would require.[24]

While no crystallographic symmetry is imposed on the nickel atoms of **14** and **15**, examination of the S–Ni–S bond angles in these structures (Table V) reveals that the symmetry of the NiS_4 fragments approaches C_2 in both cases and is not far from C_{2v} in **14**. The distortions from T_d symmetry do not follow any truly well-defined pattern. All that can be noted is the tendency for the two smallest S–Ni–S angles to be related by the twofold axis, which in turn bisects the largest S–Ni–S angle. Apparently these fragments are very susceptible to a variety of distortions along a C_2 pathway; therefore, the influence of packing effects on these geometries may be quite important. This ease of distortion was best documented for **15** since in that study the structures of four other $[(C_6H_5)_4P]_2[(C_6H_5S)_4M]$ compounds, M = Mn, Co, Zn, and Cd, were also determined. Of these five isostructural compounds, **15** showed the largest distortions from T_d symmetry.[22]

The Ni(1)–P bond lengths (average 2.1363 (4) Å) in **4a** compare reasonably well with the corresponding distances in $[\{(C_5H_5)NiP(C_6H_5)_2\}_2]$ (average 2.155 (5) Å[25]) and $[\{(C_5H_5)NiP(S)(CH_3)_2\}_2]$ (**1b**) (2.144 (4) Å), the latter containing an P–Ni–S fragment.[26] The $(C_5H_5)Ni$ moiety in **4a** resembles that reported for $[\{(C_5H_5)NiP(C_6H_5)_2\}_2]$; that is, the carbon atoms C(5) and C(7), which are closest to the NiP_2 plane, form shorter Ni–C bonds (both 2.075 (3) Å) than the other three carbons (2.115 (3)–2.143 (3) Å). The trend in the ring bond distances is also compatible with the Ni–C interactions being relatively stronger at C(5) and C(7). Furthermore, the ring is slightly nonplanar with C(5) and C(7) displaced 0.027 (3) and 0.016 (4) Å, respectively, toward Ni(1) while C(6) and C(9), which are furthest removed from the NiP_2 plane, are displaced 0.026 (3) and 0.018 (4) Å, respectively, in the opposite direction. The $(C_5H_5)NiP_2$ fragment is asymmetric as witnessed by the angle of 81.9 (3)° between the vector from the ring centroid to C(5) and the NiP_2 plane normal while angles of 72 or 90° imply C_s symmetry.

The Ni–P–S–Ni–S–P rings are nonplanar, a Cremer–Pople analysis[27] (θ = 89.88 (2)°, Φ_2 = 159.30 (2)°, Q = 1.3396 (4) Å) indicating that the conformation lies between a twist-boat and boat form. This mode of ring puckering as well as the distortions of the NiS_4 fragment leads to an overall geometry that is markedly folded (Ni(1)–Ni(2)–Ni(1′) = 125.91 (4)°) rather than the

(18) See, e.g.: Holm, R. H.; Hawkins, C. J. In *NMR of Paramagnetic Molecules*; La Mar, G. N., Horrocks, W. DeW., Jr., Holm, R. H., Eds.; Academic: New York, 1973; Chapter 7, pp 290–301.
(19) Casey, A. T.; Mitra, S. In *Theory and Applications of Molecular Paramagnetism*; Boudreaux, E. A., Mulay, L. N., Eds.; Wiley: New York, 1976; chapter 3. For a critical discussion of this argument see ref 20.
(20) Gerloch, M. *Magnetism and Ligand-Field Analysis*; Cambridge University Press: Cambridge, England, 1983; Chapter 12.4.1.
(21) Churchill, M. R.; Cooke, J.; Fennessey, J. P.; Wormald, J. *Inorg. Chem.* **1971**, *10*, 1031.
(22) Swenson, D.; Baenziger, N. C.; Coucouvanis, D. *J. Am. Chem. Soc.* **1978**, *100*, 1932.
(23) Prout, K.; Critchley, S. R.; Rees, G. V. *Acta Crystallogr., Sect. B: Struct. Crystallogr. Cryst. Chem.* **1974**, *B30*, 2305.
(24) Orgel, L. E. *An Introduction to Transition-Metal Chemistry: Ligand Field Theory*; Wiley: New York, 1960; pp 65–66.
(25) Coleman, J. M.; Dahl, L. F. *J. Am. Chem. Soc.* **1967**, *89*, 542.
(26) Lindner, E.; Bouachir, F.; Hiller, W. *J. Organomet. Chem.* **1981**, *210*, C37.
(27) Cremer, D.; Pople, J. A. *J. Am. Chem. Soc.* **1975**, *97*, 1354.

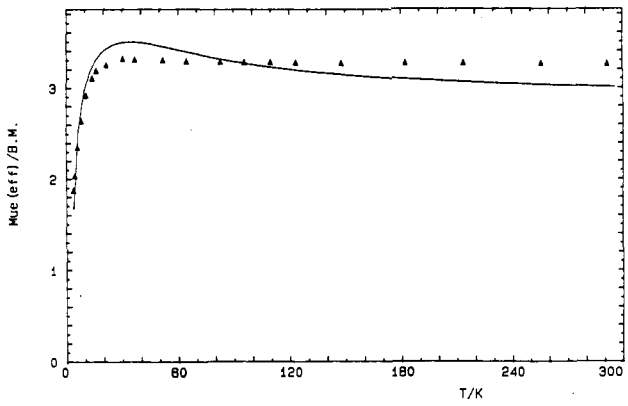

Figure 2. μ_{eff}–T diagram of $[\{(C_5H_5)Ni[P(S)(OCH_3)_2]_2\}_2Ni]$ (**4a**): (Δ) experimental values; (—) best fit with B = 550 cm^{-1}, Dq = 450 cm^{-1}, λ = −30 cm^{-1}, and k = 0.87 (see text).

Table VI. Idealization of the NiS_4 Coordination Polyhedron in **4a**

point symmetry	mean displacement of the S atoms, Å
C_2	0
C_{2v}	0.12
D_{2d}	0.42[a] / 0.40[b]
T_d	0.42

[a] Main symmetry axis is identical with twofold crystallographic axis. [b] Main symmetry axis nearly bisects the S(1)–Ni(2)–S(2) angle.

stretched geometry with colinear metal atoms often encountered in triple-decker structures. Incidently, the less severe folding of the N(1)–Ni–N(2) fragment in **14**, 154.5 (5)°, despite the irregular conformation of the Ni–S–P–N–P–S rings, is in line with the near-C_{2v} symmetry of the NiS_4 fragment.

The average P–S bond length in **4a**, 2.020 (5) Å, compares excellently with that of **14**, 2.023 (6) Å,[21] and $[\{(C_5H_5)NiP(S)(CH_3)_2\}_2]$ (**1b**), 2.015 (6) Å.[26] Longer average P–O distances are found in **4a** (1.607 (4) Å) than in $[\{(CH_3O)_2PS_2\}_2Ni]$ (1.564 (5) Å[28]) although the average O–P–O angle in the latter compound (95.9 (2)°) is smaller than that of **4a** (101 (3)°). Other distances and angles are normal.

There are no unusual intermolecular contacts, the shortest being O(1)···H(3B) (0.5 − x, 0.5 + y, 0.5 − z) at 2.52 Å. The paramagnetic nickel atoms are separated by 8.8044 (8) Å along the twofold axes. The next shortest separations are found in sheets parallel to the *bc* and *ab* planes, 9.518 (2) and 10.519 (2) Å, respectively.

Solid-State Magnetism of NiL_2 (4a). The result of the magnetochemical investigation is represented in the μ_{eff}–T diagram of Figure 2. It clearly indicates that in the temperature range 20–300 K the magnetic moment is nearly constant ($\mu_{eff} \approx 3.3\ \mu_B$) and then decreases at lower temperatures (at T = 3.8 K; $\mu_{eff} \approx 1.9\ \mu_B$). The high-temperature value of the magnetic moment is in accordance with the value reported for $[\{N[P(CH_3)_2S]_2\}_2Ni]$ (**14**).[29,30] We have tried to interpret the data in terms of a ligand field model concerning the Ni(2) centers. (It is reasonable to assume that the magnetism of the Ni(1) atoms yields only a constant contribution which is included in χ_{dia}.) Intermolecular exchange effects between the Ni(2) atoms should be negligible because the paramagnetic nickel centers are separated by 8.8–10.5 Å (see above).

The interpretation of the magnetic data is complicated by the fact that the paramagnetic Ni(2) centers possess only crystallographic C_2 point symmetry. Even if the NiS_4 unit possesses C_{2v} symmetry (see Table VI),[31] the corresponding orthorhombic ligand field model would still contain considerably more parameters than can be determined from the powder data. Therefore we have to take into consideration the higher symmetries D_{2d} or T_d. These symmetries, however, can only be achieved by much greater displacements of the sulfur atoms than in the case of C_{2v} (mean displacement 0.42 Å against 0.12 Å; see Table VI). The difference between the idealizations D_{2d} and T_d is nearly negligible, and therefore we use a simple cubic ligand field model in the fitting procedures.

Scheme I. Schematic Splitting of the d-Orbital Energies in Tetrahedral and Square-Planar Complexes as a Function of the Angular Overlap Scaling Factors e_σ and e_π

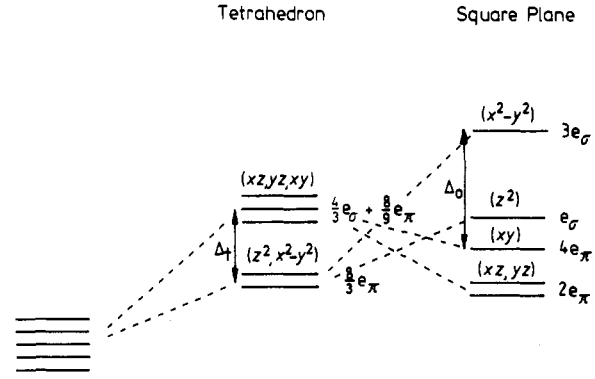

As a basis the spin-triplet terms ^3F and ^3P of the free ion are used. Taking into account the influence of a cubic ligand field and spin–orbit interaction, a susceptibility formula can be developed by applying well-known methods (e.g. ref 32–35) with the following parameters: Racah parameter B, cubic crystal field parameter Dq, spin–orbit coupling parameter λ, and the orbital reduction parameter k, which, in the framework of ligand field theory, takes into consideration metal–ligand orbital mixing[35a] and reduces the orbital contribution to the magnetic moment.

In order to simplify the calculation, the parameters B and Dq were held constant at 550 and 450 cm^{-1}, respectively. These values are estimated by comparison with those of other tetrahedral Ni(II) complexes. Model calculations show that the choice of B and Dq values within a plausible range is immaterial. Varying B by about ±50 cm^{-1} and Dq by about ±20 cm^{-1} produces hardly any change in the magnetic susceptibility. The parameters λ and k, however, strongly influence the susceptibility data. The best fit was obtained with λ = −30 cm^{-1} and k = 0.87 (see solid line in Figure 2) with a mean deviation between measured and calculated susceptibilities of about 12%. Figure 2 illustrates that in spite of the drastic simplifications the cubic model can describe the characteristic temperature dependence of the magnetic moment in a satisfactory manner. The resulting λ value of −30 cm^{-1} is strongly reduced in comparison to the free ion value of λ_0 = −315 cm^{-1} (λ/λ_0 = 0.10) and also k = 0.87 shows marked deviation from unity. Reduced values of the spin–orbit coupling parameter, however, are a characteristic phenomenon in tetrahedrally coordinated nickel(II) systems (the ratios λ/λ_0 for instance in the $[NiX_4]^{2-}$ halide systems vary between 0.41 (chloride) and 0.02 (iodide)[32]),

(28) Kastalsky, V.; McConnell, J. F. *Acta Crystallogr., Sect. B: Struct. Crystallogr. Cryst. Chem.* **1969**, *B25*, 909.
(29) Churchill, M. R.; Cooke, J.; Wormald, J.; Davison, A.; Switkes, E. S. *J. Am. Chem. Soc.* **1969**, *91*, 6518.
(30) Davison, A.; Switkes, E. S. *Inorg. Chem.* **1971**, *10*, 837.
(31) The values given in Table VI have been calculated by using a computer program that idealizes low-symmetry coordination polyhedra with as small ligand displacements as possible. Lueken, H.; Elsenhans, U.; Stamm, U.; *Acta Crystallogr., Sect. A: Found. Crystallogr.*, in press.
(32) Schläfer, H. L.; Gliemann, G. *Einführung in die Ligandenfeldtheorie*; Akademische Verlagsgesellschaft: Frankfurt am Main, 1980.
(33) Mabbs, F. E.; Machin, D. J. *Magnetism and Transition Metal Complexes*; Chapman and Hall: London, 1973.
(34) König, E.; Kremer, S. *Magnetism Diagrams for Transition Metal Ions*; Plenum: New York, 1979.
(35) (a) Gerloch, M.; Miller, J. R. *Prog. Inorg. Chem.* **1968**, *10*, 1; (b) Gerloch, M.; Slade, R. C. *J. Chem. Soc. A* **1969**, 1012, 1022; (c) Gerloch, M.; Slade, R. C. *Ligand Field Parameters*; Cambridge University Press: Cambridge, England, 1973.

Scheme II. Schematic Representation of the Destabilization of the $(C_5H_5)Ni^+$ HOMO's through Interaction with Two σ/π-Donor Ligands S[a]

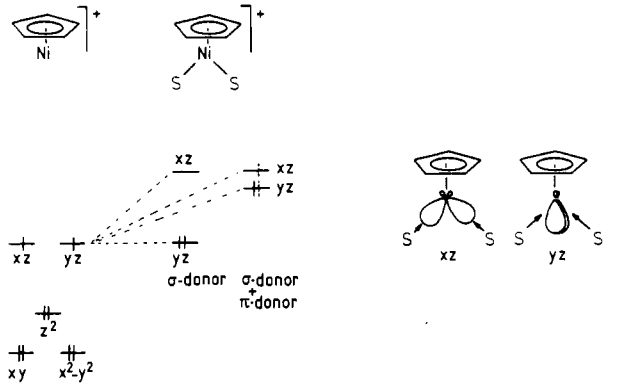

[a] *xz*, *yz*, etc. stands for the $3d_{xz}$, $3d_{yz}$, etc. derived MO's.

and small k values are also usual in tetrahedral nickel(II) complexes.[35]

Extending the ligand field model to D_{2d} symmetry does not improve the fit significantly with plausible parameter values. This result is to be expected because there is hardly any difference between the deviation of the NiS_4 coordination polyhedra from T_d and D_{2d}. The orthorhombic model, on the other hand, could markedly improve the fit as the NiS_4 polyhedron nearly has C_{2v} symmetry. One has to bear in mind, however, that the ligand field model can not be expected to fit the data to better than about 10%.[20]

Concluding Remarks

The coordination chemistry of the ligands **3a,b** presented here only resembles that of SacSac ligands in that both preferentially function as chelating rather than as bridging ligands. Electronically **3a,b** are antipodes to SacSac as the stereochemistry of their Co^{2+} and Ni^{2+} complexes has shown (i.e., $[Ni(SacSac)_2]$ and $[Co(SacSac)_2]$ *planar* vs. NiL_2 (**4a,b**) and CoL_2 (**6a**) *tetrahedral*). Comparison of the MO schemes for planar and tetrahedral transition element complexes (Scheme I) leads to the qualitative conclusion that for a d^8 configuration the planar geometry (with respect to the sterically favored tetrahedral geometry) becomes less favorable as the π-donor ability of the ligands increases with respect to their σ-donor and π-acceptor properties.[36] Therefore the tetrahedral geometry of the NiS_4 fragment in **4a** can be taken as evidence for the π-donor ability of the ligands **3a,b**.

More evidence for the strong π-donor nature of the **3a,b** ligands comes from the spin-crossover behavior of the complexes $[(C_5H_5)NiL]$ where one chelating sulfur ligand **3a** or **3b** is coordinated to a $(C_5H_5)Ni^+$ fragment. This interaction is depicted in Scheme II by using Hoffmann's frontier orbital analysis of the $(C_5H_5)Ni^+$ fragment.[37] The HOMO's of the $(C_5H_5)Ni^+$ cation are the singly occupied $3d_{xz}$ and $3d_{yz}$ derived orbitals. Interaction with two σ-donor ligands S in the *xz* plane raises the energy of d_{xz} with respect to d_{yz}.[38] The d_{yz} orbital can enter π-interactions with the ligands S. If S is a π-acceptor, d_{yz} will be stabilized, which increases the HOMO–LUMO gap. This scheme is followed by most such ligands, and it offers a rough explanation of their diamagnetism while $[Ni(C_5H_5)_2]$ possesses two unpaired electrons. Only when the ligands are good π-donors—as in the case for $[(C_5H_5)NiL]$—will the HOMO–LUMO gap become so small that a temperature-dependent singlet–triplet spin-equilibrium results. Extended Hückel calculations support this interpretation.[6]

To summarize this, we conclude that it is the pronounced π-donor properties of the ligands **3a,b** which dominate their coordination chemistry. This probably also holds for the other two sulfur ligands $[N\{P(S)R_2\}_2]^-$ and $C_6H_5S^-$, which are known to form tetrahedral NiS_4 complexes. A subtle interplay of steric requirements, spin-pairing energy, and σ-donor, π-donor, and π-acceptor properties limits however the predictability of tetrahedral NiS_4 fragments in further compounds; for example, while this moiety in $[\{N[P(S)R_2]_2\}_2Ni]$ is tetrahedral, that of $[\{HC[P(S)R_2]_2\}_2Ni]$ is square planar.[39]

Acknowledgment. We thank the Deutsche Forschungsgemeinschaft and the Fonds der Chemischen Industrie for supporting this work. Gifts of valuable chemicals from the Bayer AG and Degussa are gratefully acknowledged.

Registry No. **3a**, 87966-01-6; **3b**, 99537-67-4; **4a**, 104507-33-7; **4b**, 104507-34-8; **5a**, 104507-35-9; **5b**, 104507-36-0; **6a**, 104507-37-1; **7a**, 104531-54-6; **8a**, 104507-38-2; **9a**, 104507-39-3; **10a**, 104507-40-6; **10b**, 104507-41-7; **11a**, 104507-43-9; **12a**, 104507-44-0; **13a**, 104507-45-1; **13b**, 104507-46-2; $NiCl_2$, 7718-54-9; *trans*-$[PdCl_2(C_6H_5CN)_2]$, 15617-18-2; $CoCl_2$, 7646-79-9; $(NH_4)_2Fe(SO_4)_2$, 10045-89-3; $MnCl_2$, 7773-01-5; $Cd(OOCCH_3)_2$, 543-90-8; $Hg(OOCCH_3)_2$, 1600-27-7; $Bi(NO_3)_3$, 10361-44-1; $\{(C_5H_5)NiP(S)(CH_3)_2\}_2$, 78725-02-7; $\{(C_5H_5)NiP(S)(OCH_3)_2\}_2$, 87965-99-9; $HP(S)(OCH_3)_2$, 5930-72-3; $HP(S)(CH_3)_2$, 6591-05-5; $ClHgCH_3$, 115-09-3.

Supplementary Material Available: A stereoscopic view of the cell contents of $[\{(C_5H_5)Ni[P(S)(OCH_3)_2]_2\}_2Ni]$ (**4a**) and tables of additional bond angles, hydrogen coordinates, and anisotropic thermal parameters (4 pages); a table of $10|F_o|$ and $10F_c$ values (25 pages). Ordering information is given on any current masthead page.

(36) The angular overlap method for d^8 complexes indicates that the high-spin T_d configuration is destabilized by $^{10}/_3e_\sigma$ and stabilized by $^{16}/_9e_\pi$ with respect to the low-spin D_{4h} configuration. The actual situation is however more complex since the high-spin T_d geometry is unstable toward a Jahn–Teller distortion. See e.g.: (a) Purcell, K. F.; Kotz, J. C. *Inorganic Chemistry*; W. B. Saunders: Philadelphia, 1977; Chapter 9. (b) Burdett, J. K. *Molecular Shapes*; Wiley: New York, 1980; Chapter 11. (c) Reference 24.

(37) Lauher, J. W.; Elian, M.; Summerville, R. H.; Hoffmann, R. *J. Am. Chem. Soc.* **1976**, *98*, 3219.

(38) Incidently, the above-noted distortions in the $(C_5H_5)Ni$ fragment of **4a** may be taken as a structural validation of this orbital splitting.

(39) Davison, A.; Reger, D. L. *Inorg. Chem.* **1971**, *10*, 1967.